On the thickness of soap films: An alternative to Frankel's law

ERNST A. VAN NIEROP, BENOIT SCHEID AND HOWARD A. STONE

School of Engineering and Applied Sciences, Harvard University, Cambridge, MA 02138

(Received 1 February 2008)

The formation of soap films by vertical withdrawal from a bath is typically described by Frankel's law, which assumes rigid film "walls" and shear-like dynamics. Since most soap films have interfaces that are not rigid, and as the flow in the withdrawal of thin free films is typically extensional, we reconsider the theory of soap film formation. By assuming extensional flow dominated by surface viscous stresses we find that the film thickness scales as the two-thirds power of the withdrawal speed U. This speed dependence is also predicted by Frankel's law; the difference lies in the origin of the viscous resistance which sets the pre-factor. When bulk viscous stresses are important the speed dependence can vary between $U^{2/3}$ and U^2.

1. Introduction

It is simple to make a soap film by withdrawing a wire frame from a bath of soapy water as sketched in figure 1a. Whether demonstrating colorful interference patterns in a soap film or determining properties of an industrial foam, an accurate prediction of the soap film thickness is important. Frankel is credited with showing that if the soap film interfaces are assumed to be rigid and inextensible, then for withdrawal the film thickness h_0 varies as (Mysels *et al.* 1959)

$$\frac{h_0}{\ell_c} = 1.89 \left(\frac{\eta U}{\gamma}\right)^{2/3} = 1.89\, C_a^{2/3}\,, \tag{1.1}$$

where $\ell_c = \sqrt{\gamma/\rho g}$ is the capillary length, η is the viscosity of the liquid, U is the speed at which the film is withdrawn from the bath, γ is the surface tension and C_a is the capillary number. The derivation of (1.1) is *identical* to that used in the Landau-Levich-Derjaguin (LLD) problem where a flat plate is withdrawn from a bath of fluid as sketched in figure 1b (see e.g. de Gennes *et al.* (2004)). However, Frankel assumes that both film interfaces act as rigid plates moving up with constant speed U, hence the prefactor in (1.1) is twice as large as for the LLD result.

It is possible to examine this result using data spanning more than 40 years of work by independent research groups, as shown in figure 2. These experiments have confirmed that $h_0 \propto U^{2/3}$ over a large range of U, with deviations at both low speeds, when the film thickness $h_0 \leqslant 100$ nm and intermolecular forces play a role, and high speeds, when the film thickness saturates to the diameter of the wire frame. The spread in the pre-factor in the data in figure 2 is larger than can be attributed to the experimental error reported by the investigators and suggests that Frankel's law, with its sole viscous dependence on the shear viscosity of the liquid, may not be universally valid.

Here, we challenge the underlying assumption in Frankel's analysis that the flow is

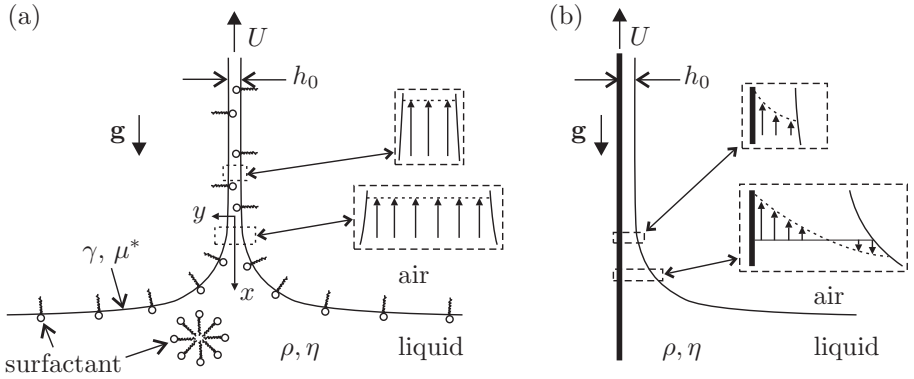

FIGURE 1. (not drawn to scale) (a) Sketch of a soap-film pulling experiment. In all reported experiments, the concentration of the surfactant is close to or above the critical micelle concentration (cmc), so micelles are present in the bulk. The flow is extensional, i.e. the velocity field u is a function of x only as illustrated by the insets. (b) Sketch of the typical LLD film-coating experiment, which can be performed with or without surfactants. The flow is shear-like, as sketched for two different positions in the film.

shear-like (as sketched in figure 1b) and suggest that an *extensional* flow with extensible film interfaces may be a better description of the physical processes that govern the thickness of a soap film during withdrawal. In particular, we account for the resistance associated with deformation of a surfactant-covered interface, through surface viscosity (Scriven 1960).

2. Alternative to Frankel's Law

Assuming that the flow in a soap film is essentially extensional (see figure 1a), and allowing for surface viscous effects, we derive a stress balance for the dynamic meniscus. The dynamic meniscus spans the region of fluid between the *static* meniscus and the film of constant thickness, and typically extends over a length scale ℓ (to be determined) where $h_0 \ll \ell \ll \ell_c$. In appendix A, we asymptotically analyze the Stokes equations for small aspect ratios $\epsilon = h_0/\ell$, using normal and tangential stress boundary conditions at the free interfaces which account for Marangoni and surface viscous stresses.

Since all of the experimental withdrawal velocities were slow (between μm/s - mm/s), and surfactant concentrations were close to or larger than the critical micelle concentration (cmc), surfactant diffusion across the film and subsequent adsorption to the interface occur more rapidly than surface stretching (see appendix A.3. for details). As a result, surface tension gradients are expected to be negligible and Marangoni stresses are not included in what is to follow. Similarly, although gravity sets the length scale and curvature of the static meniscus where fluid and surface motions are negligible, it is not a dominant source of stress in the *dynamic* meniscus due to the smallness of the film thickness. The resulting one-dimensional stress balance for the steady dynamic meniscus of thickness $h = h(x)$ is (see appendix A)

$$\underbrace{4\,\eta\,(hu_x)_x}_{O\left(\frac{\eta h_0 U}{\ell^2}\right)} + \underbrace{2\,\mu^*\,(u_x)_x}_{O\left(\frac{\mu^* U}{\ell^2}\right)} + \underbrace{\frac{\gamma}{2}\,h\,h_{xxx}}_{O\left(\frac{\gamma h_0^2}{\ell^3}\right)} = 0\,, \tag{2.1}$$

where $u = u(x)$ is the velocity in the x-direction, and $\mu^* = \mu_s + \kappa_s$ is the combination of surface shear (μ_s) and surface dilatational (κ_s) viscosities. The first term in (2.1) accounts

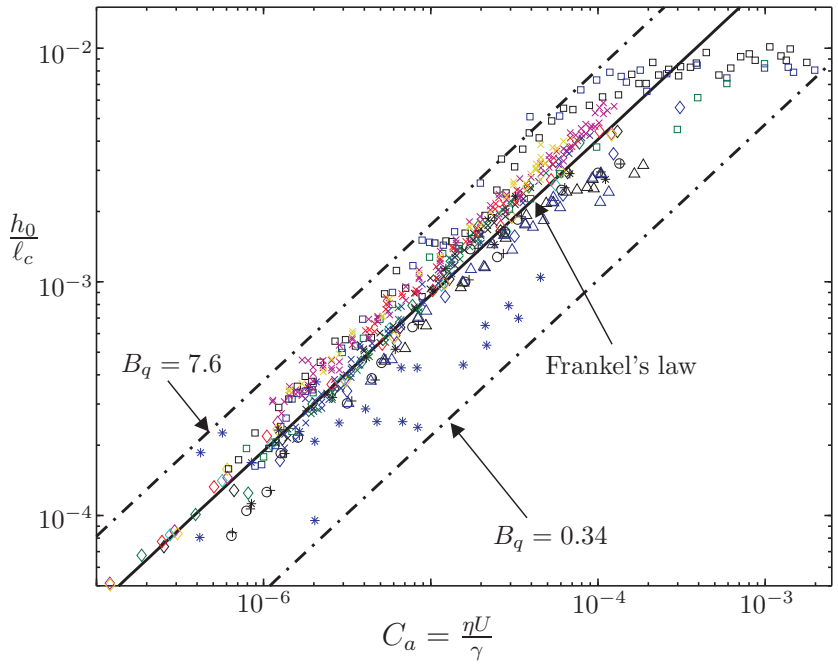

FIGURE 2. All existing data on soap film thicknesses; see table 1 for a full legend. Solid line: Frankel's law (1.1). Dash-dotted lines: full solutions to (2.4) for values of B_q that correspond to roughly 2 and $\frac{1}{4}$ times Frankel's law, respectively.

for bulk extensional stresses where the factor 4 is the Trouton ratio for viscous stretching of a Newtonian fluid sheet, the second term accounts for surface viscous stresses, and the third term accounts for stresses induced by the curvature of the interface. Both of the viscous terms are described in more detail in appendix A.1. A similar stress balance without surface viscosity but with Marangoni stresses has been used to describe drainage of a foam lamella (Breward & Howell 2002) or, including gravitational effects, a film on a retina (Braun & King-Smith 2007). By including the influence of surface viscosity we assume that the interface is *not* rigid, and we account for (surface) viscous dissipation associated with shearing or extending an interface with surfactants (Edwards *et al.* 1991).

The introduction of surface viscosity μ^* leads to two key dimensionless parameters, namely the Boussinesq number $B_q = \mu^*/(\eta\ell_c)$ and the 'surface capillary' number $C_s = \mu^* U/(\gamma\ell_c) = C_a\, B_q$. The Boussinesq number represents a balance between surface viscous stresses and (extensional) bulk viscous stresses. A balance of the viscous terms in (2.1) shows that surface viscous terms will dominate as long as $\mu^*/(\eta h_0) \equiv B_q\,\ell_c/h_0 \gg 1$, which is usually the case.

Estimates of μ^* come from measurements of κ_s which is typically orders of magnitude larger than μ_s. Since $\kappa_s \sim 10^{-6} - 10^{-3}$ Pa.m.s (e.g. Fruhner *et al.* (1999); Liu & Duncan (2006)), we expect $B_q \sim 1 - 10^3$, which emphasizes the relative importance of surface properties. Including surface viscous effects in the dynamics of soap films is therefore not uncommon, e.g. it has been used to model film drainage (Schwartz & Roy 1999; Naire *et al.* 2001), and it dominates foam relaxation times (Durand & Stone 2006).

Comparing the typical relative magnitude of the two viscous terms in (2.1), we find that the length scale of the dynamic meniscus will be set by a balance between surface viscous effects and curvature, i.e. $\ell = \gamma h_0^2/(4\mu^* U) \equiv h_0^2/(4\,\ell_c\, C_s)$. Using continuity

Symbol	Source	η mPa.s	γ mN/m	μ^* μPa.m.s	Solutions
◊	Mysels & Cox (1962)	0.9	38	5.2	0.25% commercial detergent
		0.9	31	4.5	1% comm.det.
		0.9	32	4.5	5% comm.det.
		0.9	50	5.9	0.29% SDS
		0.9	34	4.7	0.2% SDS + 0.01% dodecanol
		2.7	45	15	0.25% comm. det. + 37% glycerol
		14.5	51	64	+ 68% glycerol
+	Bruinsma *et al.* (1992)	1	33	3.3	2% (8 × cmc) SDS (70% pure)
○	Lionti-Addad & di Meglio (1992)	1.05	33	3.8	2% SDS (70% pure)
∗	Cohen-Addad & di Meglio (1994)	1.1	17	4.1	0.01% (2.6 × cmc) "fluoro" (zwitter.)
		1.3	30	1.8	0.5% (250 × cmc) $C_{12}E_5$ (nonionic)
△	Lal & di Meglio (1994)	1.25	23	3.9	4% octanoic acid
		1.24	37	4.9	4% decanoic acid
□	Adelizzi & Troian (2004)	1	37	8.4	2% SDS + 4% glycerol
		1	36	8.8	+ 8% glycerol
		1	29	5.4	2% (12 × cmc) SDBS
×	Berg *et al.* (2005)	1	50	7.1	0.08% SDS
		1	45	6.2	0.1% SDS
		1	39	6.0	0.4% SDS
		1	37	7.5	2% SDS
		1	37	7.7	2% SDS + 4% glycerol
		1	35	8.0	+ 8% glycerol

TABLE 1. Solutions used for the data shown in figure 2. All solutions are aqueous and concentrations of surfactant are reported as weight %. Viscosities and surface tensions are all as reported, except for the data from Mysels & Cox for which γ was calculated. Surface viscosities were calculated using (2.5a) after performing a best fit of the experimental data to the function $\log(h_0/\ell_c) = \frac{2}{3}\log(C_a) + f$, where f is the fitting parameter.

($u\,h = U\,h_0$ = constant) to re-write (2.1) as an ODE for h, and non-dimensionalizing with $h = h_0\,H$ and $x = \ell\,X$, we obtain

$$-2\frac{\eta\,h_0}{\mu^*}\left(\frac{H_X}{H}\right)_X - \left(\frac{H_X}{H^2}\right)_X + H\,H_{XXX} = 0\,. \tag{2.2}$$

There are two sets of boundary conditions for (2.2). On one end, the film evolves to a constant thickness, i.e. $H \to 1$ and $H_X, H_{XX} \to 0$ as $X \to -\infty$. On the other end, the film matches the curvature of a static meniscus: $H_{XX} \to \alpha$ as $X \to \infty$. Equation (2.2) is integrated once with respect to X, and the integration constant is set to zero to satisfy the boundary conditions; multiplying the result by $H^{-3/2}$ and integrating again gives

$$\frac{4\,h_0/\ell_c}{3\,B_q}H^{-3/2} + \frac{2}{5}H^{-5/2} + H^{-1/2}H_X + c = 0\,, \tag{2.3}$$

where $c = -\frac{2}{5} - \frac{4}{3}(h_0/\ell_c)\,B_q^{-1}$ to satisfy the boundary conditions. For $X \gg 1$, $H = \frac{\alpha}{2}X^2$ and substitution into (2.3) shows $\alpha = c^2/2$. Since the static meniscus has curvature $h_{xx} = \sqrt{2}/\ell_c$, then $\alpha\,h_0/\ell^2 = \sqrt{2}/\ell_c$, and we obtain

$$\frac{h_0}{\ell_c} = 2^{3/2}\left(\frac{1}{5} + \frac{2}{3}\frac{h_0/\ell_c}{B_q}\right)^{2/3} C_s^{2/3}, \tag{2.4}$$

which is our main result. Evaluating (2.4) in the limits where surface viscous effects or

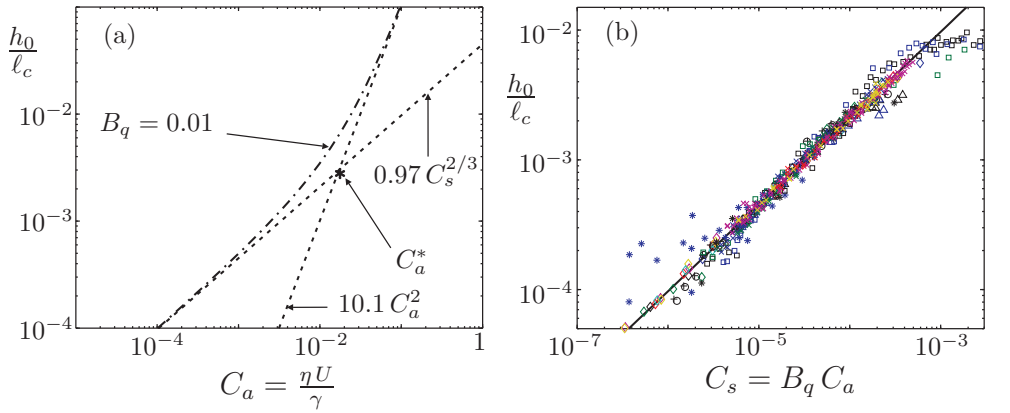

FIGURE 3. (a) Full solution (dash-dotted) and the two limits of (2.4) for $B_q = 0.01$. Note that only one of the two limits depends on B_q, and there is a transition between the limits at C_a^* as described in the text. (b) Data from figure 2 can be collapsed onto a single line corresponding to (2.4) using the fitted values for surface viscosity as reported in table 1.

bulk viscous effects dominate, respectively, gives

$$\frac{h_0}{\ell_c} = \begin{cases} 0.97\,C_s^{2/3} & \text{if } (h_0/\ell_c)\,B_q^{-1} \ll 0.3 \text{ or } C_a \ll C_a^* \qquad (2.5a) \\ 10.1\;C_a^2 & \text{if } (h_0/\ell_c)\,B_q^{-1} \gg 0.3 \text{ or } C_a \gg C_a^* \qquad (2.5b) \end{cases}$$

where C_a^* is defined as the cross-over between the limits $h_0/\ell_c \propto C_a^{2/3}$ and $h_0/\ell_c \propto C_a^2$, yielding $C_a^* \approx 0.2\,B_q^{1/2}$ as shown in figure 3a.

3. Results and Discussion

In the experiments presented in figure 2 the expected values of B_q are such that $C_a \ll C_a^*$. As a result, data that are plotted versus C_a, as in figure 2, are scattered by differences in the 'pre-factor', i.e. differences in surface viscosity as measured by B_q. The analytical result (2.4) suggests that it would make more sense to plot film thicknesses versus the surface capillary number C_s rather than C_a. If we use (2.5a) to find the surface viscosity that best fits each data set, we can collapse all existing data as shown in figure 3b. The values obtained for surface viscosity are reported in table 1; they are all of order $10^{-5} - 10^{-6}$ Pa.m.s. which is consistent with existing data albeit on the lower end of the spectrum. The possible relationship of surface viscosity to bulk shear viscosity as observed for two of the solutions used by Mysels & Cox is unclear, and certainly depends on the specific components present in the film under consideration. For *commercial* detergents it has been reported that adding glycerol can increase surface viscosity (Martin & Wu 1995), although the method used in that work only measures surface *shear* viscosities.

In conclusion, taking into account surface viscosity in an extensional flow leads to the same speed dependence for film thickness as Frankel's law, without assuming unrealistic rigid interfaces. Work is ongoing to probe the regime of low surface viscosity and large capillary number, where film thickness should scale as U^2. Additionally, we are working to better determine the role of Marangoni stresses at higher withdrawal speeds. If Marangoni stresses are indeed negligible, as assumed in this work, then measuring soap film thicknesses may become a useful method to measure surface viscosities. Other ongoing work will address the effect of adding water-soluble polymers to the film. Such

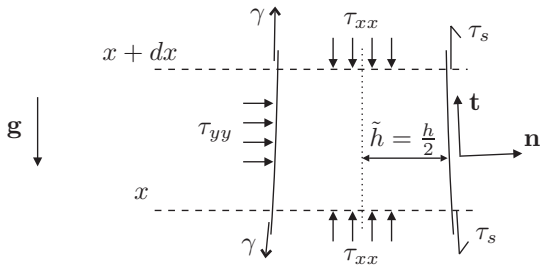

FIGURE 4. Illustration of main sources of stress in a fluid film element. For clarity surface tension is only shown on the left and surface viscous stresses are only shown on the right. Likewise, τ_{yy} acts equally and oppositely on the right film interface as well.

solutions may exhibit unusual scalings since they are generally non-Newtonian and can exhibit large extensional viscosities.

We thank the Harvard MRSEC DMR-0213805, and Unilever Research for support of this research. We thank Peter Howell for helpful conversations about thin films.

Appendix A. Derivation of the stress balance

The stress balance as shown in (2.1) is derived here along the same lines as the extensional flow derivation given by Breward (1999). We start with the Stokes equations

$$\boldsymbol{\nabla} \cdot \mathbf{u} = 0, \quad \text{and} \quad \mathbf{0} = -\boldsymbol{\nabla} p + \eta \nabla^2 \mathbf{u} - \rho \mathbf{g}, \tag{A 1}$$

as well as normal and tangential stress conditions at the free surface $y = \tilde{h} = h/2$ (see figure 4), which include the effects of a constant surface viscosity (cf. Naire *et al.* (2001)),

$$p_a + \mathbf{n} \cdot \boldsymbol{\tau} \cdot \mathbf{n} = \quad 2\mathcal{H} \left(\gamma + (\mu^s + \kappa^s) \boldsymbol{\nabla}_\mathrm{s} \cdot \mathbf{u} \right) \tag{A 2a}$$

$$\mathbf{t} \cdot \boldsymbol{\tau} \cdot \mathbf{n} = \mathbf{t} \cdot \boldsymbol{\nabla}_\mathrm{s} \left(\gamma + (\mu^s + \kappa^s) \boldsymbol{\nabla}_\mathrm{s} \cdot \mathbf{u} \right), \tag{A 2b}$$

where p_a is the ambient pressure and $\boldsymbol{\tau}$ is the fluid stress tensor, $\mathcal{H}$ is the mean curvature of the interface, $\mathbf{n}$ and $\mathbf{t}$ are the normal and tangent vectors to the free surface (see figure 4), and $\boldsymbol{\nabla}_\mathrm{s} = \boldsymbol{\nabla} - \mathbf{nn} \cdot \boldsymbol{\nabla}$ is the surface gradient operator. We denote the velocity field by $\mathbf{u} = (u, v)$ and use subscripts to indicate derivatives. The origin of the boundary terms in (A 2) is discussed in more detail in appendix A.1. Finally we note that there is a kinematic boundary condition at the free surface, $v(y = \tilde{h}) = \tilde{h}_t + u\tilde{h}_x$, and there is symmetry midway the film, i.e. $v(y = 0) = 0$ and $u_y(y = 0) = 0$. We then non-dimensionalize these equations using the following scales

$$x = \ell X, \; y = h_0 Y, \; u = u_0 U, \; v = \epsilon u_0 V, \; p - p_a = \tfrac{\eta u_0}{\ell} P,$$
$$\tilde{h} = h_0 H, \; t = \tfrac{\ell}{u_0} T, \; \gamma = \gamma_0 + \Delta\gamma \, \sigma, \tag{A 3}$$

where p_a is the ambient pressure, and σ is the non-dimensional surface tension. Expanding the equations to first order in $\epsilon = h_0/\ell$, the continuity and momentum equations are

$$U_{0_X} + V_{0_Y} = 0, \quad U_{0_{YY}} = 0, \quad V_{0_{YY}} - P_{0_Y} = 0, \tag{A 4}$$

and the boundary conditions on the free interface are

$$-P_0 + 2V_{0_Y} - 2U_{0_Y} H_X - \frac{\epsilon}{C_a} H_{XX} = 0, \quad U_{0_Y} = 0, \quad V_0 = H_T + U_0 H_X. \tag{A 5}$$

Integrating $U_{0_{YY}}$ twice with respect to Y, and applying the boundary and symmetry

conditions, we find that $U_0 = U_0(X,T)$, and thus has no Y-dependence. This result is precisely the main feature of an *extensional* flow. At this lowest order, one can find in a straightforward manner that

$$V_0 = -U_{0_X} Y, \quad \Rightarrow \quad H_T + (U_0 H)_X = 0, \quad \text{and} \tag{A 6}$$

$$P_0 = -2U_{0_X} - \tfrac{\epsilon}{C_a} H_{XX} \quad \text{at } Y = H. \tag{A 7}$$

To find the stress balance, we must work to higher order in the x-momentum and tangential stress boundary conditions,

$$U_{2_{YY}} = P_{0_X} - U_{0_{XX}} + \mathcal{G}, \tag{A 8}$$

$$U_{2_Y} = \frac{M_a}{\epsilon}\,\sigma_X + \frac{B_q}{\epsilon}\,U_{0_{XX}} - V_{0_X} - 2\,(V_{0_Y} - U_{0_X})\,H_X \quad \text{at } Y = H, \tag{A 9}$$

where $\mathcal{G} = \rho g \ell^2/(\eta u_0)$ and $M_a = \Delta\gamma/(\eta u_0)$. Integrating (A 8) once and applying (A 9) eventually yields the overall stress balance

$$\frac{M_a}{\epsilon}\,\sigma_X + \frac{B_q}{\epsilon}\,U_{0_{XX}} + 4\,(HU_{0_X})_X + \frac{\epsilon}{C_a}\,H H_{XXX} - H\,\mathcal{G} = 0, \tag{A 10}$$

or in dimensional terms (replacing $\tilde{h}$ by $h/2$),

$$2\gamma_x + 2\mu^* u_{xx} + 4\eta\,(hu_x)_x + \frac{\gamma}{2} h\,h_{xxx} - \rho g h = 0. \tag{A 11}$$

When Marangoni stresses and the gravitational term are neglected, the stress balance as shown in (2.1) is recovered.

A.1. *Derivation of the stress balance 'by inspection'*

It can be helpful to 'derive' some of the terms in (A 11) by inspection for a uni-directional flow, rather than by rigorous asymptotics. Figure 4 shows a free-body diagram for a small part of the film; surface tension, bulk viscous stresses τ_{xx}, τ_{yy} and surface viscous stresses τ_s (i.e. the deviatoric part of $\boldsymbol{\tau}_s$ below) are indicated. Curvature induced stresses ($\sim h\,(\gamma h_{xx})_x$) and Marangoni stresses ($\sim \gamma_x$) are readily constructed from the sketch. For bulk viscous stresses note that by definition

$$\tau_{xx} = -p_0 + 2\eta\,u_x, \quad \text{and} \quad \tau_{yy} = -p_0 + 2\eta\,v_y = -p_0 - 2\eta\,u_x \tag{A 12}$$

where continuity has been used in the last expression. In an extensional flow, stress in the y-direction is constant and (therefore) equal to the ambient pressure p_a. Without loss of generality, we can consider ambient pressure to be 0, so that $\tau_{yy} = 0$ and $p_0 = -2\eta\,u_x$, and it thus follows from (A 12) that $\tau_{xx} = 4\eta\,u_x$. Since fluids flow in response to stress gradients, the bulk viscous term in (A 11) is $(h\,\tau_{xx})_x$. Similarly, surface viscous stress depends on surface velocity gradients, i.e. $\tau_s \propto \mu^* u_x$, and hence the surface viscous term in (A 11) looks like $\sim \mu^*\,(u_x)_x$. Note that the factor 2 in the first two terms of (A 11) accounts for the fact that there are two surfaces.

A.2. *A note on μ^* and the lack of pure dilatation*

In an extensional flow one may be tempted to think that surface motion is dilatational, and therefore that μ^* should be replaced by κ_s in the expressions above. However, this is not so. Since the surface is expanding in one direction only (the direction of film withdrawal), it is not a purely dilatational motion. A comparison of the stress tensor for

a 3D Newtonian fluid and a 2D 'Newtonian surface' helps reveal why μ^* involves surface shear viscosity. For a Newtonian fluid, the constitutive equation for the stress is

$$\boldsymbol{\tau} = -\left(p_0 - \kappa\left(\boldsymbol{\nabla}\cdot\mathbf{u}\right)\right)\mathbf{I} + 2\eta\left(\mathbf{E} - \frac{1}{3}\boldsymbol{\nabla}\cdot\mathbf{u}\,\mathbf{I}\right), \tag{A 13}$$

where $\mathbf{E} = \frac{1}{2}\left(\boldsymbol{\nabla}\mathbf{u} + \boldsymbol{\nabla}\mathbf{u}^T\right)$ is the rate of strain tensor and κ is the 'second coefficient of friction' which relates only to dilatation of bulk fluid. In the case of incompressible flows, naturally $\boldsymbol{\nabla}\cdot\mathbf{u} = 0$ and the stress tensor simplifies. Scriven (1960) extended the ideas that go into the construction of (A 13) to surfaces. Without doing Scriven's seminal work justice, (A 13) can be recast into a 2D version for surfaces by 'replacing' the internal pressure p_0 by surface tension and using surface operators where appropriate, i.e.

$$\boldsymbol{\tau}_s = \left(\gamma + \kappa_s\left(\boldsymbol{\nabla}_\mathrm{s}\cdot\mathbf{u}\right)\right)\mathbf{I}_s + 2\mu_s\left(\mathbf{E}_s - \frac{1}{2}\left(\boldsymbol{\nabla}_\mathrm{s}\cdot\mathbf{u}\right)\,\mathbf{I}_s\right), \tag{A 14}$$

where $\mathbf{I}_s = \mathbf{I} - \mathbf{nn}$ is the surface projection operator and $\mathbf{E}_s$ is just the 2D version of $\mathbf{E}$, evaluated at the interface. For an extensional flow such as the one under consideration $\mathbf{E}_s \propto u_x$ and $\boldsymbol{\nabla}_\mathrm{s}\cdot\mathbf{u} = u_x$ so (A 14) reduces to

$$\boldsymbol{\tau}_s = \left(\gamma + \left(\kappa_s + \mu_s\right)u_x\right)\mathbf{I}_s, \tag{A 15}$$

which clearly shows why μ^* contains contributions from surface shear, even in this unidirectional extensional flow.

A.3. *Timescales of surfactant transport*

To determine the potential role of Marangoni stresses, it is useful to consider the time scales that dominate surfactant transport and adsorption, and to compare that to the rate of surface expansion (e.g. Shen *et al.* (2002)). If the surfactant moves to new parts of the interface very rapidly, then it is reasonable to expect surface tension gradients to be negligible.

When new interface is generated by stretching on a timescale of $t_s = \ell/U$, surfactant will populate the interface by diffusing there within a typical time $t_d = h_0^2/D$ and then, for surfactants shown in table 1, adsorbing in about $t_a \approx 4\cdot 10^{-4}$ s (Shen *et al.* 2002). Comparing t_s and t_d,

$$\frac{t_d}{t_s} = \frac{h_0^2\,U}{D\,\ell} \approx \frac{\ell_c\,\gamma}{\eta\,D}\,C_a^2 \approx 10^7\,C_a^2\,B_q \tag{A 16}$$

where D is the diffusion coefficient of surfactant in the bulk (of order 10^{-9} m^2/s), and we used $\ell \propto h_0^2/\left(l_c\,C_s\right)$. For the typical C_a and B_q numbers encountered in film withdrawal experiments, surface stretching is always slower than diffusion and adsorption.

REFERENCES

Adelizzi, E. A. & Troian, S. M. 2004 Interfacial slip in entrained soap films containing associating hydrosoluble polymer. *Langmuir* **20**, 7482–7492.

Berg, S., Adelizzi, E. A. & Troian, S. M. 2005 Experimental study of entrainment and drainage flows in microscale soap films. *Langmuir* **21**, 3867–3876.

Braun, R. J. & King-Smith, P. E. 2007 Model problems for the tear film in a blink cycle: single-equation models. *J. Fluid Mech.* **586**, 465–490.

Breward, C. J. W. 1999 The mathematics of foam. PhD thesis, Oxford University.

Breward, C. J. W. & Howell, P. D. 2002 The drainage of a foam lamella. *J. Fluid Mech.* **458**, 379–406.

Bruinsma, R., di Meglio, J. M., Quéré, D. & Cohen-Addad, S. 1992 Formation of soap films from polymer solutions. *Langmuir* **8**, 3161–3167.

Cohen-Addad, S. & di Meglio, J.-M. 1994 Stabilization of aqueous foam by hydrosoluble polymers 2. Role of polymer/surfactant interactions. *Langmuir* **10**, 773–778.

Durand, M. & Stone, H. A. 2006 Relaxation time of the topological T1 process in a two-dimensional foam. *Phys. Rev. Lett.* **97**, 226101.

Edwards, D. A., Brenner, H. & Wasan, D. T. 1991 *Interfacial Transport Processes and Rheology*. Boston: Butterworth-Heinemann.

Fruhner, H., Wantke, K.-D. & Lunkenheimer, K. 1999 Relationship between surface dilational properties and foam stability. *Colloids Surfaces A* **162**, 193–202.

de Gennes, P. G., Brochard-Wyart, F. & Quéré, D. 2004 *Capillarity and Wetting Phenomena: Drops, Bubbles, Pearls, Waves*. New York: Springer-Verlag.

Lal, J. & di Meglio, J.-M. 1994 Formation of soap films from insoluble surfactants. *J. Colloid Interf. Sci.* **164**, 506–509.

Lionti-Addad, S. & di Meglio, J.-M. 1992 Stabilization of aqueous foam by hydrosoluble polymers 1. Sodium dodecyl sulfate – poly(ethylene oxide) system. *Langmuir* **8**, 324–327.

Liu, X. & Duncan, J. H. 2006 An experimental study of surfactant effects on spilling breakers. *J. Fluid Mech.* **567**, 433–455.

Martin, B. & Wu, X.-I. 1995 Shear flow in a two-dimensional Couette cell: A technique for measuring the viscosity of free-standing liquid films. *Rev. Sci. Instrum.* **66**, 5603–5608.

Mysels, K. J. & Cox, M. C. 1962 An experimental test of Frankel's law of film thickness. *J. Colloid Sci.* **17**, 136–145.

Mysels, K. J., Shinoda, K. & Frankel, S. 1959 *Soap Films: Studies of Their Thinning*. New York: Pergamon Press.

Naire, S., Braun, R. J. & Snow, S. A. 2001 An insoluble surfactant model for a vertical draining free film with variable surface viscosity. *Phys. Fluids* **13**, 2492–2502.

Schwartz, L. W. & Roy, R. V. 1999 Modeling draining flow in mobile and immobile soap films. *J. Colloid Interf. Sci.* **218**, 309–323.

Scriven, L. E. 1960 Dynamics of a fluid interface: Equation of motion for Newtonian surface fluids. *Chem. Eng. Sci.* **12**, 98–108.

Shen, A. Q., Gleason, B., McKinley, G. H. & Stone, H. A. 2002 Fiber coating with surfactant solutions. *Phys. Fluids* **14**, 4055.